

DETECTION OF A SUPERNOVA SIGNATURE ASSOCIATED WITH GRB 011121¹

J. S. BLOOM², S. R. KULKARNI², P. A. PRICE^{2,3}, D. REICHART², T. J. GALAMA², B. P. SCHMIDT³, D. A. FRAIL^{2,4}, E. BERGER², P. J. McCARTHY⁹, R. A. CHEVALIER⁵, J. C. WHEELER⁶, J. P. HALPERN⁷, D. W. FOX², S. G. DJORGOVSKI², F. A. HARRISON², R. SARI⁸, T. S. AXELROD³, R. A. KIMBLE¹⁰, J. HOLTZMAN¹¹, K. HURLEY¹², F. FRONTERA¹³, L. PIRO¹⁴, & E. COSTA¹⁴

Submitted to The Astrophysical Journal (Letters), 21 March 2002

ABSTRACT

Using observations from an extensive monitoring campaign with the *Hubble Space Telescope* we present the detection, light curves, and broad-band spectral evolution of an intermediate time flux excess (a “bump” which is redder in color relative to typical afterglow emission) in the afterglow of GRB 011121, currently distinguished as the gamma-ray burst with the lowest known redshift. The red bump is remarkably well described by a redshifted Type Ic supernova, with a luminosity about half that of SN 1998bw, which occurred contemporaneously with the gamma-ray burst event. Given the simplicity of the model, we argue against alternative models for intermediate-time bumps (such as dust echoes) which require fine tuning to reproduce the observations. Instead, these results serve as compelling evidence for a massive star origin of long duration gamma-ray bursts. We further exclude the (related) supranova model and discuss the relationship between spherical core-collapse supernovae and gamma-ray bursts.

Subject headings: supernovae: general miscellaneous — gamma rays: bursts — supernovae: individual (SN 1998bw)

1. INTRODUCTION

The observational evidence for the connection of long-duration gamma-ray bursts (GRB) with massive stars (Woosley 1993) has been mounting on a variety of spatial scales. On the largest scale, GRBs have been found (so far) only in star-forming galaxies, including Ultra-Luminous IR galaxies (ULIRGS; Berger et al. 2001), and in detail, the radial distribution of GRBs follow the UV light of their hosts (Bloom et al. 2002). Further, in several instances, GRBs may lie close to or on top of star-forming complexes (e.g., Hjorth 2000; Holland & Hjorth 1999). At least a third of bursts have no detectable optical afterglows but possess strong X-ray and/or radio afterglow (the “dark” GRBs) and in the better studied cases there is direct indication of extinction along the line of sight (e.g., GRB 970828; Djorgovski et al. 2001).

The currently popular model of GRB progenitors is the

so-called “collapsar” model (Woosley 1993; MacFadyen & Woosley 1999; Hansen 1999) in which the core of a massive star collapses to a compact stellar object (such as a black hole or magnetar) which then powers the GRB while the rest of the star explodes. We expect to see two unique signatures in this scenario: a rich circumburst medium fed by the mass-loss of the massive progenitor and an underlying supernova (SN). Unfortunately broadband modeling of afterglows have not yielded firm signatures for such circumburst medium (Chevalier & Li 1999; Frail et al. 2000).

However, there has been tantalizing evidence for an underlying SN. The first association of a cosmologically-distant GRB¹⁵ with the death of a massive star was found for GRB 980326, where a clear excess of emission was observed, over and above the rapidly-decaying afterglow component. This late-time “bump” was interpreted as arising from an underlying SN (Bloom et al. 1999), since unlike the afterglow, the bump was very red. This red

¹ Based on observations with the NASA/ESA Hubble Space Telescope, obtained at the Space Telescope Science Institute, which is operated by the Association of Universities for Research in Astronomy, Inc. under NASA contract No. NAS5-26555.

² Division of Physics, Mathematics and Astronomy, 105-24, California Institute of Technology, Pasadena, CA 91125

³ Research School of Astronomy & Astrophysics, Mount Stromlo Observatory, via Cotter Rd., Weston Creek 2611, Australia

⁴ National Radio Astronomy Observatory, Socorro, NM 87801

⁵ Department of Astronomy, University of Virginia, P.O. Box 3818, Charlottesville, VA 22903-0818

⁶ Astronomy Department, University of Texas, Austin, TX 78712

⁷ Columbia Astrophysics Laboratory, Columbia University, 550 West 120th Street, New York, NY 10027

⁸ Theoretical Astrophysics 130-33, California Institute of Technology, Pasadena, CA 91125

⁹ Carnegie Observatories, 813 Santa Barbara Street, Pasadena, CA 91101

¹⁰ Laboratory for Astronomy and Solar Physics, NASA Goddard Space Flight Center, Code 681, Greenbelt, MD 20771

¹¹ Department of Astronomy, MSC 4500, New Mexico State University, P.O. Box 30001, Las Cruces, NM 88003

¹² University of California at Berkeley, Space Sciences Laboratory, CA 94720-7450

¹³ Istituto Tecnologie e Studio Radiazioni Extraterrestri, CNR, Via Gobetti 101, 40129 Bologna, Italy

¹⁴ Istituto Astro sica Spaziale, C.N.R., Area di Tor Vergata, Via Fosso del Cavaliere 100, 00133 Roma, Italy

¹⁵ GRB 980425 was associated with the nearby SN 1998bw at $z = 0.0085$ (Galama et al. 1998) but if the association is true, as we believe, then the burst is severely under-luminous (by 10^5 in energy) with respect to the distribution of other long-duration GRBs (Frail et al. 2001). This event thus appears to be a new class of GRB (e.g., Bloom et al. 1998).

color was explained as being due to metal line blanketing of the supernova spectrum blueward of 4000 Å in the restframe, a universal characteristic of supernovae in the photospheric phase.

Suggestions of intermediate-time bumps in GRB light curves have since been put forth for a number of other GRBs (Lazzati et al. 2001; Sahu et al. 2000; Fruchter et al. 2000; Björnsson et al. 2001; Castro-Tirado et al. 2001; Sokolov 2001; Dar & Rújula 2002). Most of these results are tentative or suspect, however, relying on a few mildly deviant photometric points in the afterglow light curve, and further, lack the requisite spatial resolution to separate the afterglow from the host galaxy. GRB 970228 with the characteristic SN spectral rollover is another good candidate (Reichart 1999; Galama et al. 2000).

Alternative explanations for the late-time bumps have been advanced: dust echoes (Esin & Blandford 2000; Reichart 2001) and thermal re-emission of the afterglow light (Waxman & Draine 2000). Lacking spectroscopic observations (exhibiting characteristic SN features) or multi-color observations the case for an underlying SN has not been firmly established (Reichart 2001).

It is against this background that we initiated a program with the *Hubble Space Telescope* (HST) to sample afterglow light curves at intermediate and late-times. The superb photometric stability and high angular resolution of HST are essential in separating the afterglow from the host galaxy and in constructing colors of the afterglow.

GRBs with low redshifts, $z \lesssim 1$ are particularly valuable since for such bursts the characteristic strong absorption for $\lambda \lesssim 4000$ Å (restframe) appears in the optical band and, in particular, are amenable to observations with the Wide Field Planetary Camera 2 (WFPC2). The effect of the absorption blanketing is a source with an apparent red spectrum at observer-frame optical wavelengths. Here we report on WFPC2 multi-color photometry of GRB 011121 ($z = 0.36$; Infante et al. 2001) and elsewhere we report on observations of GRB 010921 ($z = 0.451$; Price et al. 2002a). We report a multi-wavelength (radio, optical and NIR) modeling of the afterglow in the companion paper by Price et al. (2002b) (hereafter Paper II).

2. OBSERVATIONS AND REDUCTIONS

2.1. Detection of GRB 011121 and the afterglow

On 2001 November 21.7828 UT, the bright GRB 011121 was detected and localized by BeppoSAX to a 5-arcmin radius uncertainty (Piro et al. 2001a). As measured by the Ulysses satellite, the fluence in the 25–100 keV bandpass was 2×10^{-5} erg cm $^{-2}$ (Hurley et al. 2001). Subsequent observations of the error circle refined by the IPN and BeppoSAX (Hurley et al. 2001; Piro et al. 2001b) revealed a fading optical transient (OT) (Wyrzykowski et al. 2001; Stanek et al. 2001). Spectroscopic observations with the Magellan 6.5-m revealed redshifted emission lines at the OT position ($z = 0.36$), indicative of a bright, star-forming host galaxy (Infante et al. 2001) of GRB 011121.

2.2. HST Observations and reductions

For all the visits, the OT and its underlying host were placed near the serial readout register of WF chip 3 (aperture WFALL) to minimize the effect of charge transfer

(in)efficiency (CTE). The gain was set to 7 electrons DN $^{-1}$ and the typical readnoise is 5 electrons (r.m.s.).

In the first epoch, 2001 December 4–6 UT, we imaged in each filter twice at two positions dithered by 2.5 pixels (CR-SPLIT=1) each for 400s (1600s per filter; 5 orbits in total). The transient, as well as the host galaxy, was well-detected in all filters (F450W, F555W, F702W, F814W, F850LP). Given the high measured Galactic extinction toward the field (Paper II) we opted not to use the F450W (blue) filter in subsequent epochs: in epochs 2 and 3 (2001 December 14–16 UT and 2001 December 19 UT) we imaged with F555W, F702W, F814W, and F850LP (4 orbits each epoch). As the source was continuing to fade (see below), to maximize the probability of detection of the transient, we chose to concentrate our efforts in epoch 4 (2002 February 14 UT) on the F555W, F702W, and F814W filters. For this epoch, we increased the integration times in all filters and devoted 2 orbits to the F702W filter with a 6-point dither pattern to maximize the signal-to-noise on point source detection.

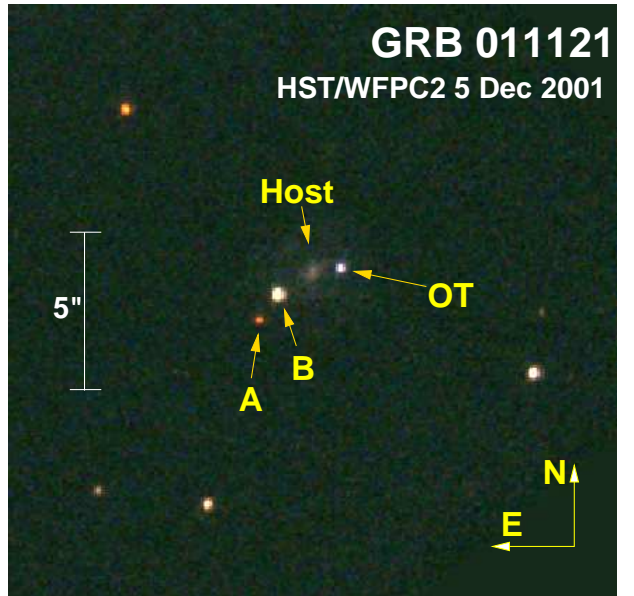


FIG. 1.— *Hubble Space Telescope* image of the field of GRB 011121 on 2001 December 4–6 UT. This false-color image was constructed by registering the final drizzled images in the F555W (blue), F702W (green) and F814W (red) filters. The optical transient (OT) is clearly resolved from the host galaxy and resides in the outskirts of the morphologically smooth host galaxy. Following the astrometric methodology outlined in Bloom et al. (2002), we find that the transient is offset from the host galaxy (883 ± 7) mas West, (86 ± 13) mas North. The projected offset is (4.805 ± 0.035) kpc, almost exactly at the half-light radius. Sources “A” and “B” are non-variable point sources that appear more red than the OT and are thus probably foreground stars.

The data were pre-processed with the best bias, dark, and flat-field calibrations available at the time of retrieval from the archive (“on-the-fly” calibration). We combined all of the images using the standard IRAF/DITHER2 package to remove cosmic rays and produce a better sampled final image in each filter. The final image scale was 70 mas pixel $^{-1}$ (SCALE=0.7 and PIXFRAC=0.8). An image of the region surrounding the transient is shown in figure 2.2. The OT was detected at better than 20σ in epochs 1–3 in all filters, and better than 5σ in epoch 4.

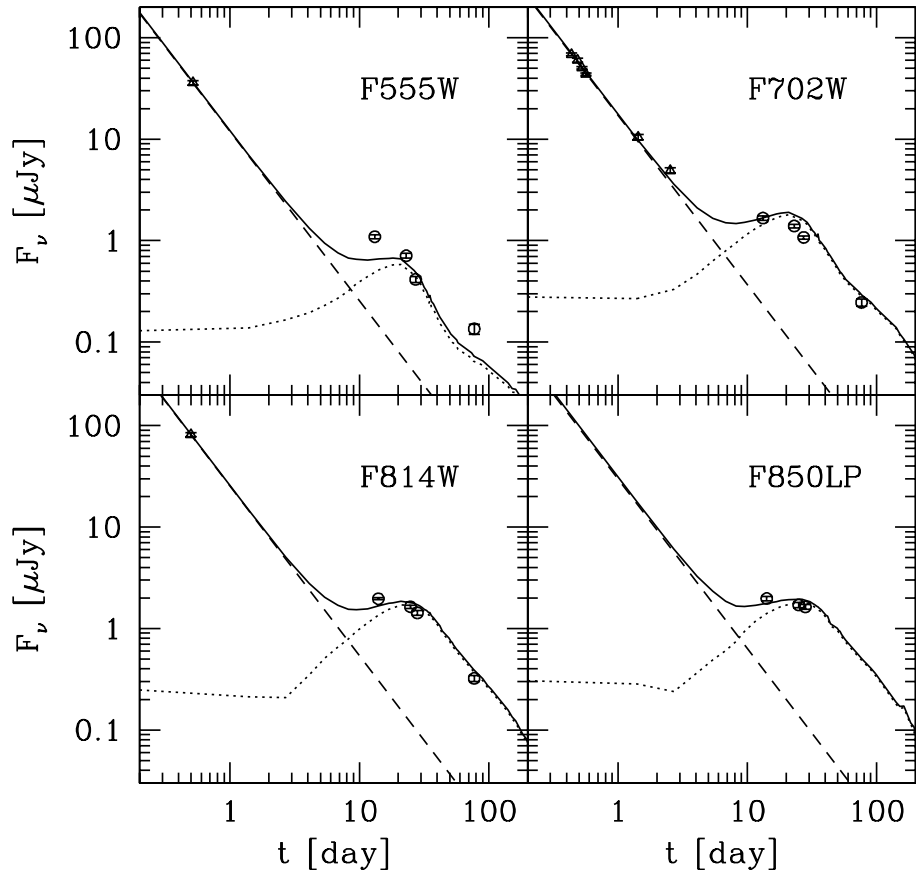


FIG. 2.— Light-curves of the afterglow and the intermediate-time red bump of GRB 011121. The circles are our HST photometry in the F555W, F702W, F814W and F850LP filters (all uncorrected for the uncertain contribution from the host galaxy) and the triangles are ground-based measurements from the literature (Olsen et al. 2001; Stanek & Wyrzykowski 2001). The dashed line is our fit to the optical afterglow (see Paper II), the dotted line is the expected flux from SN 1998bw at the redshift of GRB 011121, with foreground extinction applied and dimmed by 2/3 mag to approximately fit the data, and the solid line is the sum of the afterglow and SN components.

Given the proximity of the OT to its host galaxy, the final HST images were photometered using the IRAF/DAOPHOT package which implements PSF-fitting photometry on point-sources (Stetson 1987). The PSF local to the OT was modeled with PSTSELECT and PSF using at least 15 isolated stars detected in the WF chip 3 with an adaptive kernel to account for PSF variations across the image (VARORDER = 1). The resulting photometry, reported in table 1, was obtained by finding the flux in an $0''.5$ radius using a PSF fit. We corrected the observed countrate using the formulation for CTE correction in Dolphin (2000) with the most up-to-date parameters¹⁶; such corrections, computed for each individual exposure, were never larger than 8% (typically 4%) for a final drizzled image. We estimated the uncertainty in the CTE correction, which is dependent upon source flux, sky background, and chip position, by computing the scatter in the CTE corrections for each of the images that were used to produce the final image. The magnitudes reported in the standard bandpass filters in table 1 was found using the Dolphin prescription.

The corrected countrate was converted to flux using

the IRAF/SYNPHOT package. An input spectrum with $f_\nu = \text{constant}$ was first assumed. Then, approximate spectral indices between each filter were computed and then used to re-compute the flux and the effective wavelength of the filters. This bootstrapping converged after a few iterations. The HST photometry contains an unknown but small contribution from the host galaxy at the OT location. We attempted to estimate the contamination of the host at the transient position by measuring the host flux in several apertures at approximate isophotal levels to the OT position; the results are given in Table 1.

3. RESULTS

In figure 2 we plot the measured fluxes from our four HST epochs in the F555W, F702W, F814W and F850LP filters. We also plot measurements made at earlier times ($0.5 \text{ d} < t < 3 \text{ d}$) with ground-based telescopes and reported in the literature. These magnitudes were converted to fluxes using the zero-points of Fukugita et al. (1995) and plotted in the appropriate HST filters. Corrections for color effects between the ground-based filters and HST filters were taken to be negligible for the purpose of this

¹⁶ See http://www.noao.edu/staff/dolphin/wfpc2_calib/

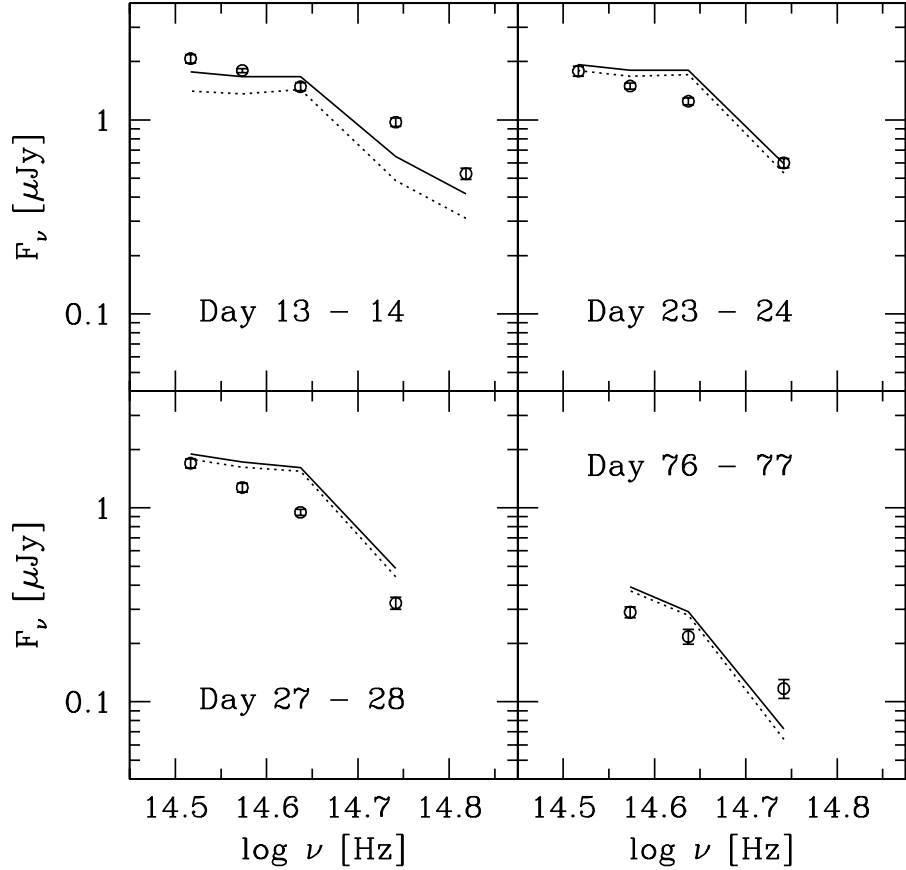


FIG. 3.— The spectral flux distributions of the red bump at the time of the four HST epochs. The circles are our HST measurements, including an uncertain contribution from the host galaxy (mainly affecting only the fourth epoch). The dotted line is the SFD of SN 1998bw transformed to the redshift of GRB 011121, reddened and scaled down by 2/3 mag (see text). The solid line is the sum total of the afterglow component (assuming no “jet” break) and the SN component. The afterglow dominates the total only in the first epoch.

exercise.

The estimated contribution from the afterglow is heavily weighted by the available data: our ground-based data (and those reported in the literature so far) are primarily at early times. Roughly, over the first week, the afterglow exhibits a simple power law decay. The afterglow contribution derived from our NIR data and optical data from the literature (see Paper II) is shown by the dashed line in each panel.

Garnavich et al. (2002) drew attention to an excess of flux (in R -band), at epoch 13 d, to that expected from the power-law extrapolation of early-time afterglow emission and they suggested the excess to arise from an underlying SN. As can vividly be seen from our multi-color data, the excess is seen in all bands.

We used the light curve of the well studied Type Ic supernova SN 1998bw (Galama et al. 1998; McKenzie & Schaefer 1999) and derived the rest-frame and de-reddened (after correcting for the foreground extinction of $A_V = 0.19$ mag; Galama et al. 1998) spectral flux distribution. The resulting low-resolution spectrum was then redshifted to $z = 0.36$ and scaled by d_L^2 (see Schmidt et al. 1998), assuming a flat Λ cosmology with $H_0 = 65 \text{ km s}^{-1} \text{ Mpc}^{-1}$ and $\Omega_M = 0.3$ and then subject to a foreground extinction

with $A_V = 1.14$ mag derived from optical/NIR modeling of the early afterglow (Paper II).

The excess emission can be satisfactorily accounted for by the light curve of SN 1998bw provided it is dimmed by about 2/3 mag (see Figure 2). Some minor deviations are apparent, particularly in the F555W band, but such discrepancies are entirely expected (see §4). Discrepancies at late times may also be attributed to the uncertain contribution from the host galaxy to the measured flux.

In figure 3 we plot the spectral flux distributions (SFDs) of the intermediate-time bump at the four HST epochs. The dotted curve is the SFD of SN 1998bw transformed as described above. The solid curve includes contribution from the afterglow. The consistency between the measurements and the SN is reasonable, but some differences are observed, as expected.

Using our adopted fluxes for the host galaxy contribution to the afterglow light (table 2) we find a decay between epochs 3 and 4 of $\delta m_{F555W} = 0.035 \text{ mag day}^{-1}$, $\delta m_{F702W} = 0.065 \text{ mag day}^{-1}$, $\delta m_{F814W} = 0.077 \text{ mag day}^{-1}$ in the restframe of GRB 011121. Using the results from McKenzie & Schaefer (1999) and Galama et al. (1998), between the same two epochs, SN 1998bw faded with $\delta m_V = 0.049 \text{ mag day}^{-1}$ and $\delta m_I = 0.036 \text{ mag day}^{-1}$. Between these

epochs type Ic/Ib supernovae rapidly decline for about 15 days after peak, then fade more slowly as the light begins to be powered by the radioactive decay of cobalt. The late-time decline rates of Ib/Ic appear to vary greatly and so the rough consistency between SN1998bw and the light curve of GRB011121 is heartening.

4. DISCUSSION AND CONCLUSIONS

We have presented unambiguous evidence for a red, transient excess above the extrapolated light curve of the afterglow of GRB 011121. We suggest that the light curve and spectral flux distribution of this excess appears to be well represented by a bright supernova. While we have not yet explicitly compared the observations to the expectations of alternative theories (dust, echoes, thermal re-emission from dust, etc.) the simplicity of the supernova model—requiring only a (physically motivated) adjustment in brightness—is a compelling argument to accept our hypothesis. We note that this supernova model implies a stellar explosion which occurred contemporaneously with GRB 011121. In this respect, the “supernova” model (which posits a stellar explosion months to years before the GRB event; Vietri & Stella 1999) is excluded by these observations.

Apart from establishing the connection of GRBs to collapsars these observations allow us to begin to address the details of the GRB explosion mechanism. Specifically, until now, GRBs have been viewed, particularly in their energetics, entirely via their γ -ray emission and the afterglow emission. We have had little knowledge whether the energy coupled to the supernova explosion dominates the overall explosive yield. Below we briefly describe new diagnostics made possible by detailed studies of the SN component.

As summarized in MacFadyen et al. (2001), the progenitors must lack extensive envelopes otherwise the jet may stall before reaching the high Lorentz factors required to produce bursts of γ rays. Thus, in the collapsar model, one expects to see underlying SNe of type Ib or Ic. Ordinary Ib/Ic SNe appear to show a wide dispersion in the peak luminosity (Iwamoto et al. 1998). Why such diversity exists is not fully understood, though the observed range is likely attributable to the diversity in ejecta mass and the mass and distribution of nickel mass.

For SNe associated with GRBs there will be additional complications for the following reason. It is now generally accepted that GRBs are not spherical explosions and are, as such, usually modeled as a jetted outflow. Frail et al. (2001) model the afterglow of GRBs and have presented a compilation of opening angles, θ , ranging from less than a degree to 30 degrees and a median of 4 degrees. If GRBs

have such strong collimation then it is not reasonable to assume that the explosion which explodes the star will be spherical. We must be prepared to accept that the SN explosion is extremely asymmetric and consequent diversity in the light curves.

This entirely expected diversity can account for both the scale factor difference between the SN component seen here and in SN 1998bw (which has been argued to be not a member of the cosmologically located GRBs) as well as the differences between the spectral flux densities (SFD) seen in figure 3. These SFD differences can be minimized by allowing for an adjustable overall scale factor for each epoch. However, given the above discussion, such detailed fitting is not appropriate at this point.

There has been a significant discussion in the literature as to the degree which the central engine in GRBs will affect the overall explosion of the star (Khokhlov et al. 1999; Höflich et al. 1999). These models currently have focused primarily on the hydrodynamics and lack the radiative modeling necessary to compare observations to the models.

Observationally, the next frontier lies in spectro-polarimetric studies. Such observations will provide the most definitive proof for the collapsar model and allow us to map out the 3-D velocity field of the exploding star. As shown by GRB 011121 the SN component is bright enough to undertake observations with the largest ground-based telescopes.

We end by noting the following curious point. The total energy yield of a GRB is usually estimated from the gamma-ray fluence and an estimate of θ (see Frail et al. 2001). Alternatively the energy in the afterglow is used (e.g., Piran et al. 2001). However, for GRB 011121, the energy in the SN component (scaling from the well-studied SN 1998bw) is likely to be comparable or even larger than that seen in the burst or the afterglow. In view of this, the constancy of the γ -ray energy release is even more mysterious.

J. S. B. is a Fannie and Hertz Foundation Fellow. F. A. H. acknowledges support from a Presidential Early Career award. S. R. K. and S. G. D. thank the NSF for support. R. S. is grateful for support from a NASA ATP grant. R. S. and T. J. G. acknowledge support from the Sherman Fairchild Foundation. CW acknowledges support from NASA grant NAG59302. Support for Proposal number HST-GO-09180.01-A was provided by NASA through a grant from Space Telescope Science Institute, which is operated by the Association of Universities for Research in Astronomy, Incorporated, under NASA Contract NAS5-26555.

REFERENCES

Berger, E., Kulkarni, S. R., and Frail, D. A. 2001, ApJ, 560, 652
 Björnsson, G., Hjorth, J., Jakobsson, P., Christensen, L., and Holland, S. 2001, ApJ (Letters), 552, L121
 Bloom, J. S., Kulkarni, S. R., and Djorgovski, S. G. 2002, accepted to AJ, astro-ph/0010176
 Bloom, J. S. et al. 1999, Nature, 401, 453
 Bloom, J. S., Kulkarni, S. R., Harrison, F., Prince, T., Phinney, E. S., and Frail, D. A. 1998, ApJ (Letters), 506, L105
 Castro-Tirado, A. J. et al. 2001, A&A, 370, 398
 Chevalier, R. A. and Li, Z.-Y. 1999, ApJ (Letters), 520, L29
 Dar, A. and Rújula, A. D. 2002, astro-ph/0008474
 Djorgovski, S. G., Frail, D. A., Kulkarni, S. R., Bloom, J. S., Odewahn, S. C., and Diercks, A. 2001, ApJ, 562, 654
 Dolphin, A. E. 2000, PASP, 112, 1397
 Esin, A. A. and Blandford, R. 2000, ApJ (Letters), 534, L151
 Frail, D. A. et al. 2001, ApJ (Letters), 562, L55
 —. 2000, ApJ, 534, 559
 Fruchter, A., Vreeswijk, P., Hook, R., et al. 2000, GCN notice 752
 Fukugita, M., Shimasaku, K., and Ichikawa, T. 1995, PASP, 107, 945
 Galama, T. J. et al. 2000, ApJ, 536, 185
 —. 1998, Nature, 395, 670

Garnavich, P. M., Holland, S. T., Jha, S., Kirshner, R. P., Bersier, D., and Stanek, K. Z. 2002, GCN notice 1273

Höflich, P., Wheeler, J. C., and Wang, L. 1999, ApJ, 521, 179

Hansen, B. M. S. 1999, ApJ (Letters), 512, L117

Hjorth, J. 2000, GRB Circular Network, 753

Holland, S. and Hjorth, J. 1999, A&A, 344, L67

Holtzman, J. A., Burrows, C. J., Casertano, S., Hester, J. J., Trauger, J. T., Watson, A. M., and Worthey, G. 1995, PASP, 107, 1065

Hurley, K., Cline, T., Guidorzi, C., Montanari, E., Frontera, F., and Feroci, M. 2001, GCN notice 1148

Infante, L., Garnavich, P. M., Stanek, K. Z., and Wyrzykowski, L. 2001, GCN notice 1152

Iwamoto, K. *et al.* 1998, Nature, 395, 672

Khokhlov, A. M., Höflich, P. A., Oran, E. S., Wheeler, J. C., Wang, L., and Chtchelkanova, A. Y. 1999, ApJ (Letters), 524, L107

Lazzati, D. *et al.* 2001, A&A, 378, 996

MacFadyen, A. I. and Woosley, S. E. 1999, ApJ, 524, 262

MacFadyen, A. I., Woosley, S. E., and Heger, A. 2001, ApJ, 550, 410

McKenzie, E. H. and Schaefer, B. E. 1999, PASP, 111, 964

Olsen, K., Brown, M., Schommer, R., and Stubbs, C. 2001, GCN Notice 1157

Piran, T., Kumar, P., Panaiteescu, A., and Piro, L. 2001, ApJ (Letters), 560, L167

Piro, L. *et al.* 2001a, GCN notice 1147

—. 2001b, GCN notice 1149

Price, P. A., Schmidt, B. P., and Kulkarni, S. R. 2002a, GCN notice 1259

Price, P. A. *et al.* 2002b, in preparation

Reichart, D. E. 1999, ApJ (Letters), 521, L111

—. 2001, ApJ, 554, 643

Sahu, K. C. *et al.* 2000, ApJ, 540, 74

Schmidt, B. P. *et al.* 1998, ApJ, 507, 46

Sokolov, V. V. 2001, astro-ph/0107399

Stanek, K. Z., Garnavich, P. M., and Wyrzykowski, L. 2001, GCN notice 1151

Stanek, K. Z. and Wyrzykowski, L. 2001, GCN Notice 1160

Stetson, P. B. 1987, PASP, 99, 191

Vietri, M. and Stella, L. 1999, ApJ (Letters), 527, L43

Waxman, E. and Draine, B. T. 2000, ApJ, 537, 796

Woosley, S. E. 1993, ApJ, 405, 273

Wyrzykowski, L., Stanek, K. Z., and Garnavich, P. M. 2001, GCN notice 1150

TABLE 1
LOG OF HST IMAGING OF THE OPTICAL TRANSIENT OF GRB 011121

Filter	Δt^a (days)	Int. Time (sec)	λ_{eff}^b (Å)	$f_{\nu}(\lambda_{\text{eff}})^b$ (μJy)	Vega Magnitude ^c (mag)
Epoch 1					
F450W	13.09	1600	4678.52	0.551 ± 0.037	$B = 24.867 \pm 0.073$
F555W	13.16	1600	5560.05	0.996 ± 0.049	$V = 23.871 \pm 0.056$
F702W	13.23	1600	7042.48	1.522 ± 0.072	$R = 23.211 \pm 0.054$
F814W	14.02	1600	8110.44	1.793 ± 0.042	$I = 22.772 \pm 0.032$
F850LP	14.15	1600	9159.21	1.975 ± 0.103	
Epoch 2					
F555W	23.03	1600	5630.50	0.647 ± 0.035	$V = 24.400 \pm 0.061$
F702W	23.09	1600	7002.71	1.271 ± 0.051	$R = 23.382 \pm 0.048$
F814W	24.83	1600	8105.05	1.495 ± 0.053	$I = 22.982 \pm 0.043$
F850LP	24.96	1600	9166.39	1.708 ± 0.100	
Epoch 3					
F555W	27.24	1600	5711.00	0.378 ± 0.027	$V = 25.071 \pm 0.076$
F702W	27.30	1600	7043.85	0.981 ± 0.036	$R = 23.697 \pm 0.044$
F814W	28.10	1600	8164.90	1.301 ± 0.070	$I = 23.157 \pm 0.061$
F850LP	28.16	1600	9188.39	1.635 ± 0.092	
Epoch 4					
F555W	77.33	2100	5604.61	0.123 ± 0.014	$V = 26.173 \pm 0.118$
F702W	76.58	4100	7042.09	0.224 ± 0.019	$R = 25.264 \pm 0.092$
F814W	77.25	2000	8149.18	0.294 ± 0.020	$I = 24.762 \pm 0.073$

^aMean time since GRB trigger on 21.7828 Nov 2001 UT.

^bEffective wavelength of the filter based upon the observed spectral flux distribution of the transient at the given epoch. The flux is given at this effective wavelength in an 0''5 radius. We estimate the contribution of the host galaxy to be $f_{\nu}(F450W) = (0.098 \pm 0.039) \mu\text{Jy}$, $f_{\nu}(F555W) = (0.087 \pm 0.027) \mu\text{Jy}$, $f_{\nu}(F702W) = (0.127 \pm 0.026) \mu\text{Jy}$, $f_{\nu}(F814W) = (0.209 \pm 0.059) \mu\text{Jy}$, and $f_{\nu}(F850LP) = (0.444 \pm 0.103) \mu\text{Jy}$. To correct these numbers to “infinite aperture” multiply the fluxes by 1.096 (Holtzman et al. 1995). These fluxes have not been corrected for Galactic and host extinction.

^cTabulated brightnesses in the Vega magnitude system ($B_{\text{Vega}} = 0.02 \text{ mag}$, $V_{\text{Vega}} = 0.03 \text{ mag}$, $R_{\text{Vega}} = 0.039 \text{ mag}$, $I_{\text{Vega}} = 0.035 \text{ mag}$; Holtzman et al. 1995). Subtract 0.1 mag from these values to get the infinite aperture brightness. These magnitudes have not been corrected for Galactic and host extinction.